BIROn - Birkbeck Institutional Research Online

Targeting of AMSH to Endosomes Is Required for Epidermal Growth Factor Receptor Degradation[*]

Yu May Ma[‡§], Emmanuel Boucrot[‡§1], Judit Villén[§], El Bachir Affar[¶], Steven P. Gygi[§], Heinrich G. Göttlinger[||], and Tomas Kirchhausen[‡§2]

From the [‡]CBR Institute for Biomedical Research, [§]Department of Cell Biology, [¶]Department of Pathology, Harvard Medical School, Boston, Massachusetts 02115 and the [||]Program in Gene Function and Expression, University of Massachusetts Medical School, Worcester, Massachusetts 01605

To reach the lysosomes, down-regulated receptors such as the epidermal growth factor receptor must first be sorted into internal vesicles of late endosomes (multivesicular bodies), a ubiquitin-dependent event that requires the coordinated function of the endosome sorting complex required for transport (ESCRT) proteins. Here we report that CHMP3, an ESCRT-III complex component, and associated molecule of SH3 domain of STAM (AMSH), a deubiquitinating enzyme, interact with each other in cells. A dominant-negative version of CHMP3, which specifically prevents targeting of AMSH to endosomes, inhibits degradation but not internalization of EGFR, suggesting that endosomal AMSH is a functional component of the multivesicular body pathway.

Mono-ubiquitination is a post-translational signal for sorting internalized membrane proteins into invaginated membranes within the multivesicular bodies (MVB)[3] of late endosomes (reviewed in Refs. 1 and 2). The sorted proteins are then transferred to lysosomes, where they are degraded. This ubiquitin-dependent sorting requires the coordinated function of a number of molecules that are conserved from yeast to mammals and collectively referred to as class E Vps proteins, themselves being either components or associated proteins of the four known ESCRT complexes (ESCRT-0, ESCRT-I, ESCRT-II, and ESCRT-III) (reviewed in Ref. 3). This system is also co-opted by many enveloped viruses, such as human immunodeficiency virus-1 and Ebola, to bud from the plasma membrane and thus escape from their host cells (4–8).

Pathways of ubiquitin-directed protein degradation include a deubiquitination step for ubiquitin recycling. Of the 17 deubiquitinating enzymes present in yeast, Doa4 is the only one that is functionally linked to the MVB pathway as its deletion leads to accumulation of several membrane proteins on the limiting membrane of MVB (9, 10). Human cells contain nearly 100 gene products whose sequences indicate a potential for deubiquitinating activity (11–13). Two of the verified deubiquitinating enzymes, associated molecule of SH3 domain of STAM (AMSH) and ubiquitin-specific protease Y (UBPY), appear to function in the mammalian MVB pathway. Despite their distinct catalytic domains (14, 15), AMSH and UBPY share several characteristic features. Both proteins bind to the SH3 domain of STAM, a component of ESCRT-0 (16, 17), and both strongly colocalize with endosomes when their catalytic site is made inactive by a single point mutation (15, 18). Whether these enzymes have critical functions in the MVB pathway remains to be established as knocking down AMSH using siRNA results in moderate enhancement, rather than inhibition, of epidermal growth factor receptor (EGFR) degradation (15, 19). In contrast, knocking down UBPY using siRNA leads to inhibition of EGFR degradation as well as decreased levels of Hrs and STAM, which had been shown to be crucial for EGFR down-regulation (19, 20).

In the course of a search for molecular partners of the ESCRT-III component CHMP3, the human homologue of yeast Vps24, we found evidence for a strong interaction with AMSH. We determined that the N-terminal portion of AMSH, which does not include the STAM-binding sequence, was necessary for its interaction with CHMP3. Removal of this region or the STAM-binding sequence did not affect the endosomal localization of AMSH. Furthermore, expression of a dominant-negative version of CHMP3, which was not targeted to endosomes and did not affect the endosomal localization of the other ESCRT-III components but was still capable of interacting with AMSH, prevented AMSH from targeting to endosomes; under these conditions, the degradation of activated EGFR was strongly inhibited, although its internalization was normal. As a complementary approach to confirm the role of AMSH on EGFR degradation, we used RNA interference to knock down AMSH and found that although endocytosis of activated EGFR remained normal, its degradation was also inhibited. From these observations, we conclude that AMSH is an important participant in MVB pathway degradation of EGFR and perhaps other ubiquitinated endocytosed proteins as well.

[1] A Human Frontier Science Program Long-Term Fellow.
[2] To whom correspondence should be addressed: CBR Institute for Biomedical Research and Dept. of Cell Biology, Harvard Medical School, 200 Longwood Ave., Boston, MA 02115. Tel.: 617-278-3140; Fax: 617-278-3131; E-mail: Kirchhausen@crystal.harvard.edu.

[3] The abbreviations used are: MVB, multivesicular body; ESCRT, endosome sorting complex required for transport; EGF, epidermal growth factor; EGFR, EGF receptor; AMSH, associated molecule of SH3 domain of STAM; UBPY, ubiquitin-specific protease Y; siRNA, small interfering RNA; EGFP, enhanced green fluorescent protein; mRFP, monomeric red fluorescent protein; GST, glutathione S-transferase; HA, hemagglutinin; MS, mass spectrometry.

EXPERIMENTAL PROCEDURES

Plasmids—Human CHMP3 (BC004419) and CHMP5 (B1914173) cDNAs were purchased from Resgen and Open Biosystems, respectively. They were sequenced and subcloned into the pOZ-N vector (a gift from Dr. Y. Shi, Harvard Medical School), which also encodes the human interleukin-2 receptor. Human AMSH (BC007682) cDNA was purchased from Open Biosystems, sequenced, and subcloned into the pEGFP-C1 vector (Clontech) to create EGFP-AMSH. All deletion mutants of EGFP-AMSH were generated by PCR mutagenesis. The internal deletion of EGFP-AMSH (Δ235–239) was introduced by following the QuikChange site-directed mutagenesis strategy (Stratagene). The pmRFP-C1 plasmid was constructed by replacing the EGFP fragment of pEGFP-C1 with two tandem copies of monomeric red fluorescent protein (mRFP) sequence (21). Various fragments of CHMP3 were amplified by PCR and inserted into pGEX-4T or pmRFP-C1 vectors to generate GST or mRFP fusion proteins. FLAG-Vps4AE$_{228}$Q and FLAG-CHMP4A were described previously (6). Human CHMP2A (BC 002502), CHMP6 (BC 010108), and CHMP3 cDNAs were purchased from Open Biosystems and subcloned into the pBJ5 vector to create the FLAG-tagged CHMP2A, CHMP3 and CHMP6 constructs, respectively.

Purification and Mass Spectrometry Analysis of CHMP-binding Proteins—Purification of CHMP3- or CHMP5-binding proteins was carried out as described previously with the following modifications (22, 23). First, recombinant retroviruses carrying a bicistronic mRNA containing open reading frames of both interleukin-2 receptor and FLAG-HA-tagged human CHMP3 or CHMP5 were produced from 293T cells and were used to transduce HeLa cells. Next, the infected HeLa cells were sorted using magnetic beads conjugated with anti-interleukin-2 receptor monoclonal antibody, and the resulting stable cell lines were propagated in suspension. Cytosol was generated from 4 liters of cells by hypotonic lysis and ultracentrifugation at $100,000 \times g$ for 1 h at 4 °C. Finally, the CHMP3- or CHMP5-bound proteins were purified from the cytosol using anti-FLAG M2 and anti-HA 12CA5 monoclonal antibody-conjugated agarose beads (Sigma) sequentially, and bound proteins were fractionated on a 4–20% gradient SDS-PAGE as revealed by silver staining.

The bands corresponding to the most prominent proteins and from similar regions of the gel but corresponding to the DJ-1 (control) sample were excised, digested with trypsin, and sequenced by tandem mass spectrometry (LC-MS/MS). The tryptic peptides were separated by reverse-phase using a microcapillary C18 column (125 μm $\times$ 18 cm) and analyzed on-line with a hybrid linear ion trap-ion cyclotron resonance Fourier transform instrument (LTQ-FT, Thermo Finnigan, San Jose, CA). Full MS^2 scans were followed by 10 MS/MS spectra corresponding to the 10 most abundant ions. MS spectra were searched using Sequest algorithm, and peptide matches to the data base were filtered to ensure less than 1% false-positives hits. The sequences were AVTITDLR, AEEL-KAELLK, FQETGFFK, EYTEYNEEK, SLKPGALSNSESIP-TIDGLR, NEFTITHVLIPK, MASIYSEEGNIEHAFILYNK, YITLFIEK, QQQLEQEQFHAFEMIR, and NMAIQQELE-

KEK for AMSH and TAQEHDKRDPVVAYYCR, LYAMQTG-MKIDSK, MFLYADNEDR, LYAMQTGMK LMDQLEALKK, ATYIHNCLK LMDQLEALK, YAGSALQYEDVSTAVQ-NLQ, and QLGDNEAITQEIVGCAHLENYALK for Lip5, respectively.

GST Pulldown—Cos7 cells (transfected with FuGENE 6) were used for the pull-down assays. Cells transiently expressing the various EGFP-AMSH proteins were lysed with TGH buffer (50 mM HEPES (pH 7.5), 10% glycerol, 1% Triton X-100, Complete protease inhibitor tablet (Roche Applied Science)). The soluble fractions were then mixed with lysates from *Escherichia coli* expressing various GST-CHMP3 proteins and captured with glutathione-Sepharose beads (Amersham Biosciences) after a 3-h incubation at 4 °C. Beads were collected by low speed centrifugation ($1,000 \times g$ for 5 min) and washed five times with phosphate-buffered saline. Beads were boiled, and bound proteins were fractionated by SDS-PAGE. 10% of total input and 100% of the captured AMSH proteins were revealed by Western blot analysis with anti-EGFP (Santa Cruz Biotechnology, B2) antibody. The amount of GST and GST-CHMP3 fusion proteins captured by the beads was verified by Coomassie Blue staining.

Small Interfering RNA—HeLa cells were transfected using Oligofectamine (Invitrogen) with either one of two different human AMSH-specific siRNA duplexes (sense 5'-UUACAAAU-CUGCUGUCAUUUU-3' (15) or sense 5'-GGUAGCACAACA-GAAGCAGUU-3' purchased from Dharmacon) 24 h after seeding at ~30% confluency. The effects of AMSH depletion on EGFR internalization and degradation were followed 3 days after transfection with the single cell-based assay described below.

Immunofluorescence Microscopy—Cos7 cells were transfected using FuGENE 6 (Roche Applied Science), fixed with 3% paraformaldehyde after 10–12 h, and processed for immunofluorescence staining (24). Antibodies were purchased from Sigma (anti-FLAG M2), Santa Cruz Biotechnology (anti-EEA1), and Genentech (anti-EGFR 13A9) or received as a gift from V. Horejsi (anti-CD63). Fluorescently labeled secondary antibodies were purchased from Molecular Probes. Fluorescent images were obtained with a $\times$100 objective lens using a fluorescent Zeiss microscope configured with a spinning disk confocal head or with a $\times$40 objective lens using an upright fluorescent Zeiss microscope including a spherical aberration correction system under control of SlideBook 4 (Intelligent Imaging Innovations, Inc) for the degradation and internalization experiments.

EGFR Degradation Assay—His$_6$-tagged human EGF was expressed in *E. coli* and purified using nickel-nitrilotriacetic acid chromatography. HeLa cells transfected with siRNA oligonucleotides or Cos7 cells transfected with plasmid constructs encoding for mRFP, mRFP-CHMP3-(151–220), and mRFP-CHMP3-(151–222) in a 12-well format were serum-starved for 2 h at 72 or 12 h after transfection. The cells were then incubated with 250 ng/ml EGF at 37 °C for 5 min or 2 h followed by three washes with phosphate-buffered saline (room temperature) and immediate fixation. Cells were permeabilized with 0.05% saponin dissolved in phosphate-buffered saline including 1% bovine serum albumin and then incubated with the EGFR antibody 13A9 (dissolved in phosphate-buffered saline and 1%
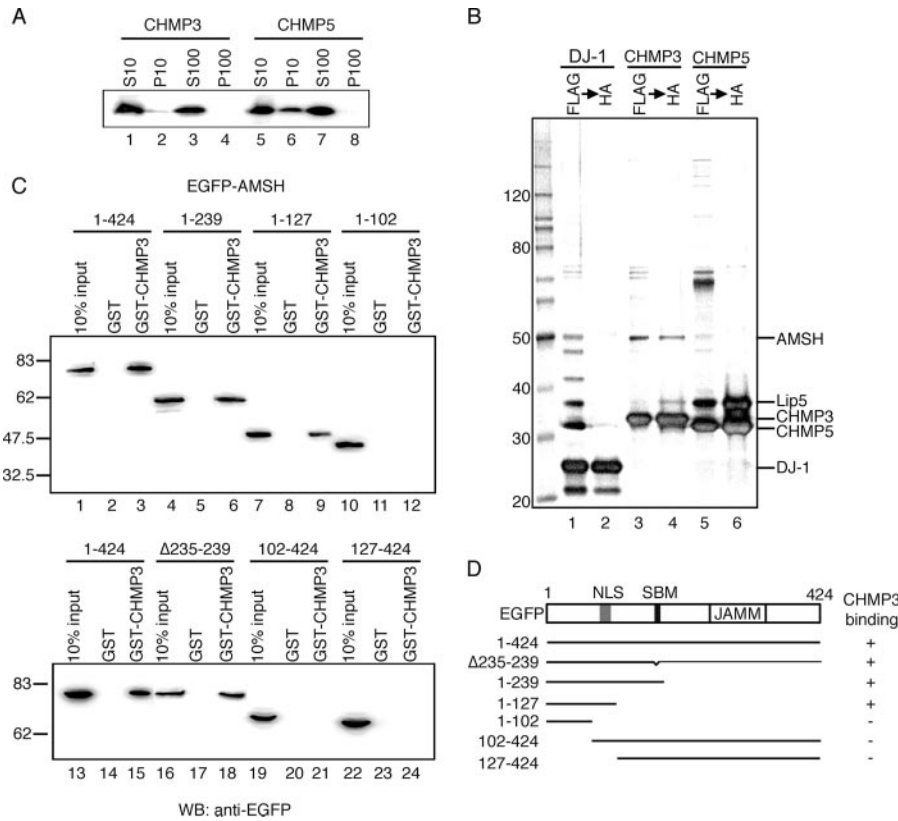
FIGURE 1. **Interaction of AMSH with CHMP3.** *A*, subcellular fractionation of HeLa cells stably expressing FLAG-HA-DJ-1, FLAG-HA-CHMP3, and FLAG-HA-CHMP5. Cells were hypotonically lysed with TGH buffer and subjected to centrifugation at 10 kg and 100 kg. Tagged proteins in each fractions were detected by Western blot using an anti-HA antibody. *B*, purification and mass spectrometry analysis of CHMP3- and CHMP5-binding proteins. Cells were lysed, and their cytosolic fractions were subjected to sequential immunoprecipitations using FLAG and HA antibody-conjugated resins. Aliquots from the proteins eluted from the beads, corresponding to the 2% of the first and 10% of the second immunoprecipitations, were fractionated by SDS-PAGE. The proteins associated with CHMP3 or CHMP5 were revealed by silver stain, and the cut bands were subjected to mass spectrometry sequence analysis. The identified proteins are indicated. *C*, mapping the CHMP3-binding region on AMSH by a GST pull-down system. Cos7 cells transiently expressing full length and mutants of EGFP-AMSH were lysed, and the soluble fraction were mixed with either GST or GST-CHMP3 followed by incubation with glutathione beads. The beads were boiled, and released proteins were fractionated by SDS-PAGE and visualized by Western blot (*WB*) analysis using an anti-EGFP antibody. The lanes show 100% of the captured EGFP-AMSH proteins and 10% of total input. *D*, schematic representation of EGFP-AMSH showing the position of its nuclear localization signal (*NLS*; 112–127), the STAM-binding motif (*SBM*; 231–239), and the JAB1/MPN/Mov34 metalloenzyme motif (*JAMM*; 323–369) involved in deubiquitination. The drawing also presents a summary of the pull-down results obtained in this study.

mass spectrometry to identify proteins interacting with CHMP3 and CHMP5, the human homologues of yeast Vps24 and Vps60, respectively (26–28). Both CHMP3 and CHMP5 proteins were tagged at their N termini with the FLAG and HA epitopes placed in tandem and stably expressed in HeLa cells. The cells were disrupted by hypotonic lysis followed by a low speed spin to remove the nuclear fraction. The analysis was performed on the high speed supernatant fraction corresponding to the cytosol since most of CHMP3 and CHMP5 are cytosolic (Fig. 1*A*). The most abundant proteins eluted from the FLAG/HA antibody-conjugated beads had SDS-PAGE mobilities corresponding to ~32–35 kDa; these proteins were CHMP3 and CHMP5, as confirmed by mass spectrometry (Fig. 1*B*, *lanes 3–6*). CHMP3 co-purified with an ~50 kDa protein, identified as human AMSH based on 10 matching peptide sequences (Fig. 1*B*, *lanes 3* and *4*). AMSH is a STAM-binding deubiquitinating enzyme (15, 29). CHMP5 co-purified with an ~38 kDa protein, identified as human Lip5 from the sequence match of nine peptides (Fig. 1*B*, *lanes 5* and *6*). The interactions of CHMP5-Lip5 and of their yeast counterparts Vps60-Vta1 were reported recently and thus were not pursued further (26, 30, 31). As a negative control for specificity of this purification approach, we analyzed the eluate from cells stably expressing double-tagged cytosolic DJ-1 (reviewed in Ref. 32), an oncogene that links to Parkinson disease and modulates oxidative stress, and verified that AMSH and Lip5 specifically associate with CHMP3 and CHMP5, respectively (Fig. 1*B*, *lanes 1* and *2*).

The interaction of epitope-tagged CHMP3 with endogenous AMSH was subsequently confirmed in a pull-down experiment using bacterially expressed GST-CHMP3 and cytosolic extracts from Cos7 cells transiently expressing EGFP-AMSH. As expected, EGFP-AMSH was detected only in association with GST-CHMP3 but not with GST alone (Fig. 1*C*, *lanes 1–3* and *13–15*). Thus, this assay allowed us to map the binding region for CHMP3 on AMSH using a series of deletion mutants of EGFP-AMSH (Fig. 1*D*). The N-terminal portion of AMSH-(1–239) bound CHMP3 as efficiently as the full-length AMSH-(1–424) (Fig. 1*C*, *lanes 4–6*). In contrast, smaller fragments (1–127 and 1–102) displayed weaker or undetectable associations (Fig. 1*C*, *lanes 7–12*). Truncations of the N-terminal portion of

bovine serum albumin) followed by a goat anti-mouse Alexa Fluor-647 secondary antibody. The total fluorescence signal within each cell was quantified using Slidebook 4 by masking out the fluorescent signals corrected by the background. 50–60 cells were analyzed for each experimental condition.

EGFR Internalization Assay—HeLa or Cos7 cells were transfected and starved as described for the EGFR degradation assay. The cells were then incubated with 50 μg/ml anti-EGFR antibody (13A9) at 37 °C for 10 min in the presence or absence of 250 ng/ml EGF (25). The cells were then fixed, permeabilized, and stained with Alexa Fluor-594 goat anti-mouse antibody (25). Image analysis was done following the same procedure used for the EGFR degradation assay. 30–40 cells were analyzed for each experimental condition.

RESULTS

AMSH Specifically Interacts with CHMP3—We used a double epitope tag purification approach combined with

AMSH Is Required for EGFR Degradation

AMSH (102–424 and 127–424) failed to interact with GST-CHMP3, indicating that the first 127 residues of AMSH are essential for association with CHMP3 (Fig. 1*C*, *lanes 19–24*). Moreover, the interaction with STAM was dispensable for the AMSH-CHMP3 association as the deletion mutant Δ235–239 lacking the STAM-binding site (16) bound CHMP3 as efficiently as the full-length AMSH (Fig. 1*C*, *lanes 16–18*).

The Simultaneous Interactions of AMSH with CHMP3 and STAM Are Not Essential for Its Endosomal Localization—We first confirmed that brief expression (10–12 h) in Cos7 cells of EGFP-AMSH resulted in the same distribution to endosomes, the plasma membrane, cytosol, and the nucleus (Fig. 2*A*), as shown previously in HeLa cells (15). EGFP-AMSH colocalized with early endosomes marked with EEA1, as reported previously (15), but not to late endosomes labeled with CD63 (Fig. 2*A*).

We next examined the contribution of association with STAM and with CHMP3 to the endosomal localization of AMSH, judging by the extent of colocalization between various EGFP-AMSH mutants and EEA1 (Fig. 2*B*). The AMSH fragment lacking the residues required for STAM association (EGFP-AMSH Δ235–239) (17) was targeted to early endosomes. Likewise, the AMSH fragment lacking the binding site for CHMP3 (EGFP-AMSH 127–424) was also recruited to EEA1-labeled endosomes. Taken together, these results confirmed that binding to STAM or to CHMP3 is not sufficient for the endosomal targeting of AMSH (33).

Overexpression of CHMP3-(151–222) Disrupts the Endosomal Localization of AMSH—Having demonstrated that mutations in AMSH preventing its association with either STAM or CHMP3 were not sufficient to mislocalize AMSH from endosomes, we sought another approach to alter the endosomal targeting of AMSH by overexpressing a truncated cytosolic form of CHMP3 (CHMP3-(151–222)) that still interacts with AMSH. As a control, we used CHMP3-(151–220) that fails to interact with AMSH (34).

We first compared the intracellular localization of EGFP-AMSH in Cos7 cells when co-expressed with CHMP3-(151–220) or CHMP3-(151–222) fused with two copies of mRFP (Fig. 3*A*). In the presence of overexpressed mRFP-CHMP3-(151–220), EGFP-AMSH retained a punctate endosomal pattern, partially localized to the EEA1 compartment, presumably due to recruitment by endogenous full-length CHMP3, STAM, and clathrin. In contrast, in the presence of overexpressed mRFP-CHMP3-(151–222), EGFP-AMSH lost its punctate pattern and became cytosolic. Expression of an ATPase-defective version of the mammalian Vps4A, $Vps4E_{228}Q$, induces the formation of enlarged hybrid organelles called class E compartments in which various ESCRT proteins are accumulated as their recycling is dependent on the ATPse activity of Vps4 (35–37). AMSH was also trapped in the class E compartments in the presence of CHMP3-(151–220) but remained cytosolic and excluded from these enlarged organelles in the presence of CHMP3-(151–222) (Fig. 3*B*). As an essential control for these experiments, we demonstrated that overexpression of the CHMP3 fragments did not affect the endosomal targeting of other ESCRT-III components. This was done by expression of either one of the truncated CHMP3 fragments together with
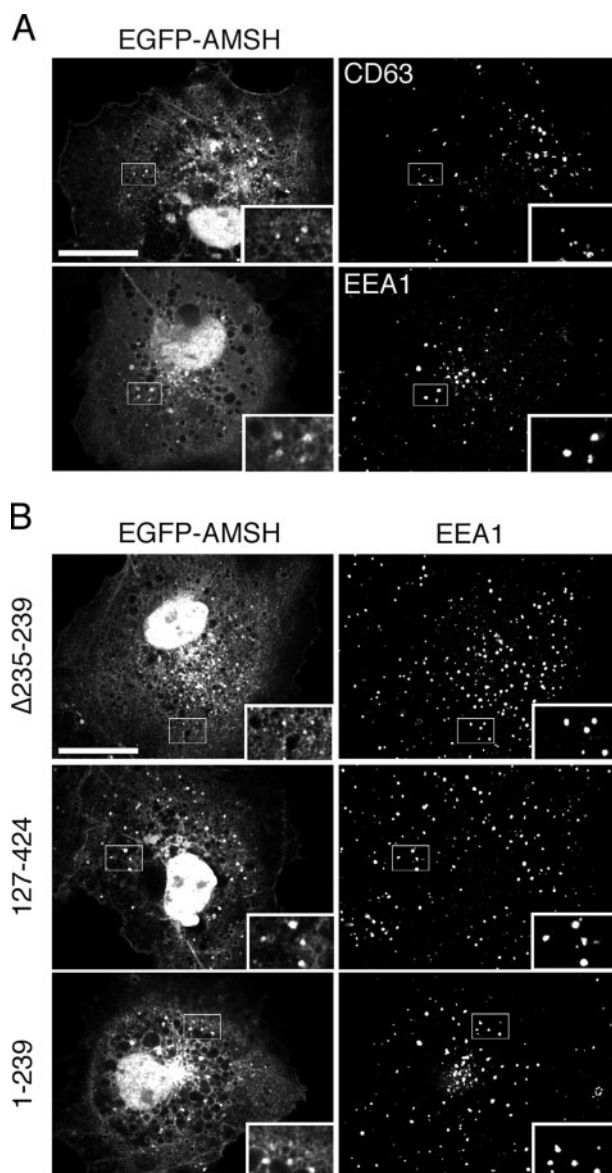
FIGURE 2. **AMSH localized to early endosomes.** *A*, Cos7 cells transiently expressing full-length EGFP-AMSH were fixed and stained with antibodies specific for EEA1 or CD63 12 h after transfection. *B*, Cos7 cells transiently expressing different truncated mutants of EGFP-AMSH were fixed and stained with anti-EEA1 antibody 12 h after transfection. All images show a confocal plane corresponding to the middle sector of the cell. *Boxed areas* are shown at higher magnification; *arrowheads* represent instances of colocalization. *Scale bar*, 20 μm.

FLAG-tagged full-length CHMP2A, CHMP3, CHMP4A, or CHMP6 and $Vps4E_{228}Q$ (used here to facilitate visualization). As shown in the examples in Fig. 3*C*, targeting of the four ESCRT-III components to the class E compartment was not affected. Therefore, CHMP3-(151–222) acted as a dominant-negative mutant and specifically prevented AMSH from localizing to endosomes (Fig. 3*A*) or to the endosome-originated class E compartment (Fig. 3*B*).

Mislocalization or Depletion of AMSH Inhibits EGFR Degradation but Not Internalization—Although the substrate specificity of AMSH is unknown, its endosomal localization suggests that it might play a role in the MVB pathway to facilitate the sorting and degradation of internalized receptors such as
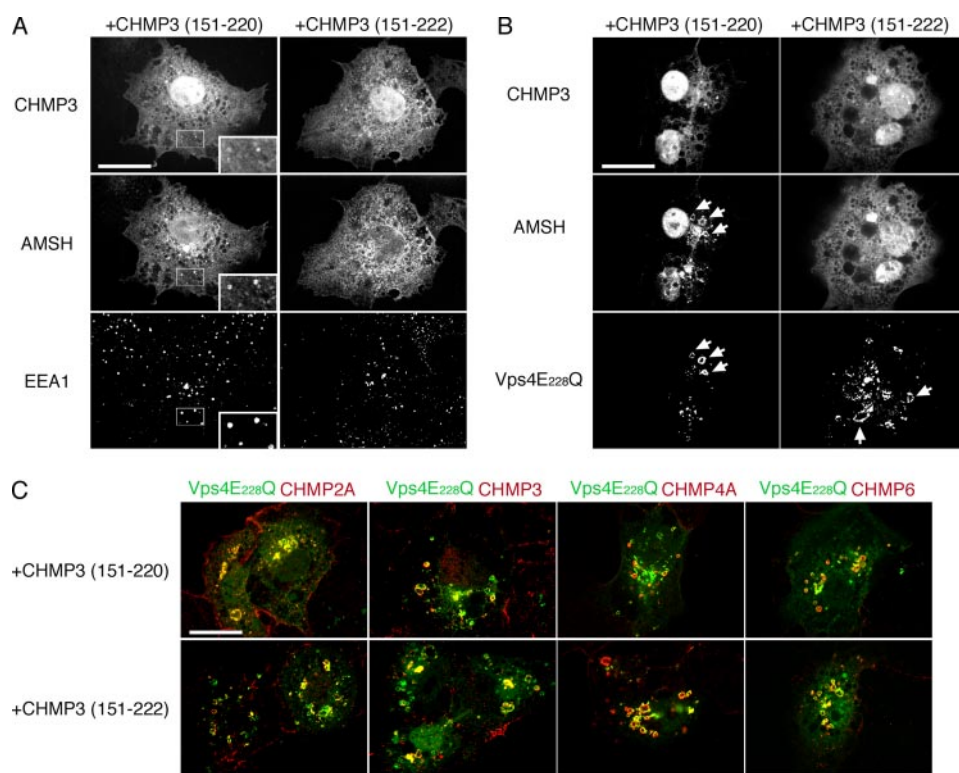
FIGURE 3. **Overexpression of CHMP3-(151–222) disrupts the endosomal localization of EGFP-AMSH.** *A*, Cos7 cells were co-transfected with EGFP-AMSH and mRFP-CHMP3-(151–220) or mRFP-CHMP3-(151–222) using a 1:2 DNA ratio and fixed 10 h after transfection. *B*, Cos7 cells were triple transfected with EGFP-AMSH, FLAG-Vps4$_{228}$Q, and mRFP-CHMP3-(151–220) or mRFP-CHMP3-(151–222) using a 1:2:2 DNA ratio. At 10 h after transfection, the cells were fixed and stained with an anti-FLAG antibody. The Vps4E$_{228}$Q-induced class E compartment is indicated with *arrows*. *C*, Cos7 cells were triple transfected with EGFP-Vps4E$_{228}$Q, mRFP-CHMP3-(151–220), or mRFP-CHMP3-(151–222), and FLAG-CHMP2, -4, or -6 using a 1:2:1 DNA ratio. At 10 h after transfection, the cells were fixed and stained with an anti-FLAG antibody. All images show a confocal plane corresponding to the middle section of the cell. *Boxed areas* are shown at a higher magnification; *arrowheads* represent instances of colocalization. *Scale bar*, 20 μm.

EGFR. Thus, we used a single cell imaging assay (26, 38) to determine whether the degradation of EGFR activated by binding to its ligand was affected in any way by preventing AMSH targeting to endosomes by mRFP-CHMP3-(151–222) overexpression (Fig. 3*A*, *right panel*). In control cells expressing mRFP only, in which AMSH was properly targeted to endosomes, EGFR was internalized normally (Fig. 4, *right panel*), and about 67% of total EGFR was degraded following 2 h of stimulation with EGF (weak punctate signal of internalized EGFR in Fig. 5*A*, *right panel* and the corresponding quantification in Fig. 5*B*). EGFR was internalized (Fig. 4) and degraded (Fig. 5) to a similar degree in cells expressing CHMP3-(151–220), which did not affect the endosomal localization of AMSH (Fig. 3*A*). In contrast, expression of CHMP3-(151–222), which causes the uncoupling of AMSH from endosomes (Fig. 3*A*), dramatically reduced EGFR degradation (Fig. 5), although the internalization was not affected (Fig. 4). The amount of EGFR present at the cell surface prior to EGF treatment was the same in all conditions (Fig. 4, *left panels*), showing that expression of the CHMP3 constructs and the mislocalization of AMSH was of no consequence for the traffic of EGFR to the cell surface.

It is possible, however, that a mechanism different from endosomal mistargeting of AMSH is responsible for the effects just described. To complement the mislocalization studies, we used an RNA interference-based approach to examine the effects of AMSH depletion on the internalization and degradation of activated EGFR using the single cell imaging assay (Fig. 6). Degradation (Fig. 6*A*, *right panels*, and 6*B*, corresponding quantification) but not internalization (Fig. 6*A*, *middle panels*) of EGFR was strongly inhibited in cells transfected for 3 days with either one of two different siRNA oligonucleotides specific for AMSH, These observations provide further evidence pointing toward an important role of AMSH in mediating EGFR degradation through the MVB pathway.

DISCUSSION

Our work provides further evidence for an interaction recently described between the deubiquitinating enzyme AMSH and CHMP3 (39), a component of the ESCRT-III complex. We also found that failure to target AMSH to endosomes by overexpression of a dominant-negative mutant form of CHMP3, which can still bind AMSH but does not localize to endosomes, impairs the degradation of internalized EGFR. This observation suggests that removal of ubiquitin by AMSH either from components of the ESCRT machinery or from internalized EGFR is important for receptor down-regulation. Presumably, AMSH also has a similar role for other membrane proteins that are degraded through the MVB pathway.

The AMSH-CHMP3 interaction provides a direct link between a mammalian deubiquitinating enzyme and the ESCRT-III complex. In contrast, the yeast deubiquitinating enzyme Doa4 that is functionally associated with the MVB pathway is linked only indirectly with the ESCRT-III complex. In that case, the direct contact is between Doa4 and Bro1, a protein whose association with endosomes depends on the ESCRT-III protein Snf7 (yeast orthologue of mammalian CHMP4) (40).

There seem to be at least three ways by which targeting of AMSH to endosomes is achieved. AMSH can interact with STAM (17, 29), CHMP3 (Ref. 39 and this work), and clathrin (39). Some form of coordinated interactions is required, however, since AMSH is found in endosomes containing clathrin but does not appear to colocalize with other clathrin-containing structures at the plasma membrane or within the perinuclear region (Ref. 15 and this work). Targeting of AMSH to early endosomes (Fig. 3*A*) requires its N-terminal region (Fig. 3*B*), which includes binding sites for CHMP3 and for STAM, whose endosomal localization in turn depends on its association with
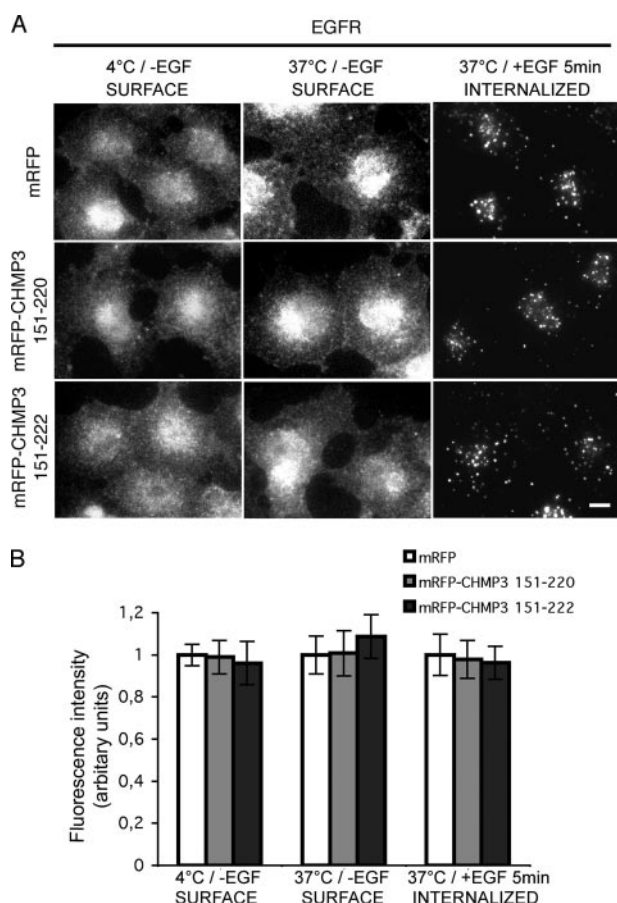
FIGURE 4. **Overexpression of CHMP3-(151–222) does not affect EGFR internalization.** *A*, 12 h after transfection with the indicated cDNA constructs, Cos7 cells were serum-starved in Dulbecco's modified Eagle's medium for 2 h. The cells were then incubated briefly (10 min) with the same medium supplemented with 50 μg/ml anti-EGFR antibody (13A9) in the absence or presence of 250 ng/ml EGF (25). All of the preceding steps were carried at 37 °C. This incubation was ended by rapidly washing the cells with Dulbecco's modified Eagle's medium kept at 4 °C followed by an acid wash step to remove surface-bound antibody applied only to the samples not treated with EGF. The cells were then fixed, permeabilized, and incubated with a fluorescently tagged Alexa Fluor-488 secondary antibody (*middle* and *right panels*). The fluorescent haze (*middle panels*) corresponds to EGFR present at the surface of cells not stimulated with EGF; the punctate pattern (*right panels*) shows the EGFR that internalized in response to EGF treatment. A similar set of cells, but not incubated with EGF, was directly transferred to 4 °C, stained with 5 μg/ml anti-EGFR antibody, fixed, and stained with the secondary antibody (*left panel*); the fluorescence haze in these images reflects the basal level of EGFR present at the cell surface. Representative images are shown. *Scale bar*, 20 μm. *B*, quantification of EGFR internalization from the immunofluorescent images. 30–40 cells expressing mRFP (*white*), CHMP3-(151–220) (*light gray*), or CHMP3-(151–222) (*dark gray*) were used for analysis; the specific fluorescent signal of each cell was determined by removing away the background signal (masking step, Slidebook 4). Data represent average signals normalized to the control sample (mRFP) ± standard error. No statistical differences (Student's *t* test) were observed between any of the experimental conditions in the amounts of surface or internalized EGFR.

Hrs (41). Because the AMSH-STAM or AMSH-CHMP3 interactions alone can still support endosomal targeting, removal of either one of these interactions cannot be used to study the effect of endosomal mislocalization on AMSH function (Fig. 2*B*). Thus, the strategy pursued here of mislocalizing AMSH is by the squelching effect of overexpressing a truncated mutant of CHMP3 that can still interact with AMSH but prevents its endosomal localization. For this approach to be valid, however, it was essential to show that the endosomal localization of other
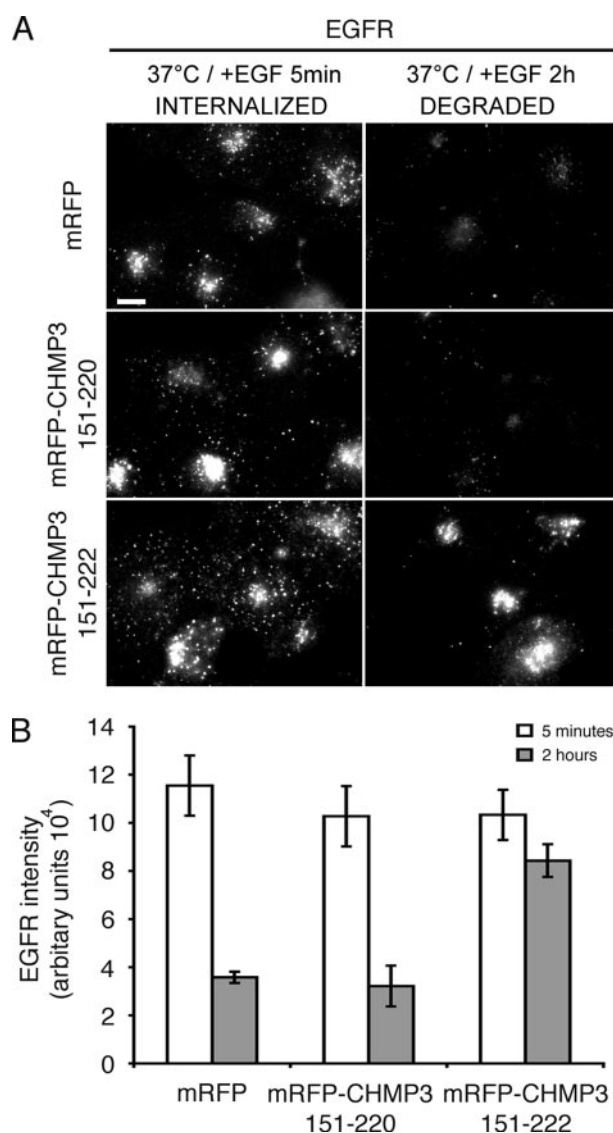

FIGURE 5. **Overexpression of CHMP3-(151–222) inhibits EGFR degradation.** *A*, Cos7 cells were serum-starved for 2 h and treated with EGF (250 ng/ml) for either 5 min or 2 h at 12 h after transfection. Cells were fixed, permeabilized, and stained with an anti-EGFR antibody (13A9). Representative images are shown. *Scale bar*, 20 μm. *B*, quantification of total EGFR from the immunofluorescent images. 50–60 transfected cells were masked as in Fig. 4*B*, and the total fluorescent intensity of the EGFR was quantified for each of the cells using Slidebook4 and expressed as average ± standard error of the mean. The statistical significance was calculated using the Student's *t* test.

ESCRT-III components remains normal upon overexpression of the CHMP3 fragment (Fig. 3*C*).

We discovered that overexpression of CHMP3-(151–222), which interacts with AMSH, acted as a dominant-negative mutant for the endosomal localization of AMSH, presumably by forming a complex with AMSH that prevents it from being targeted to endosomes (Fig. 3*A*). Furthermore, overexpression of CHMP3-(151–222) inhibited EGFR degradation without affecting its internalization (Figs. 4 and 5). In contrast, overexpression of the slightly smaller CHMP3-(151–220) had no detectable effect on the endosomal localization of AMSH or on EGFR degradation (Figs. 3*A* and 4, *A* and *B*). It is possible that overexpression of CHMP3-(151–222), but not CHMP3-(151–220), sequesters other binding partners of CHMP3 besides
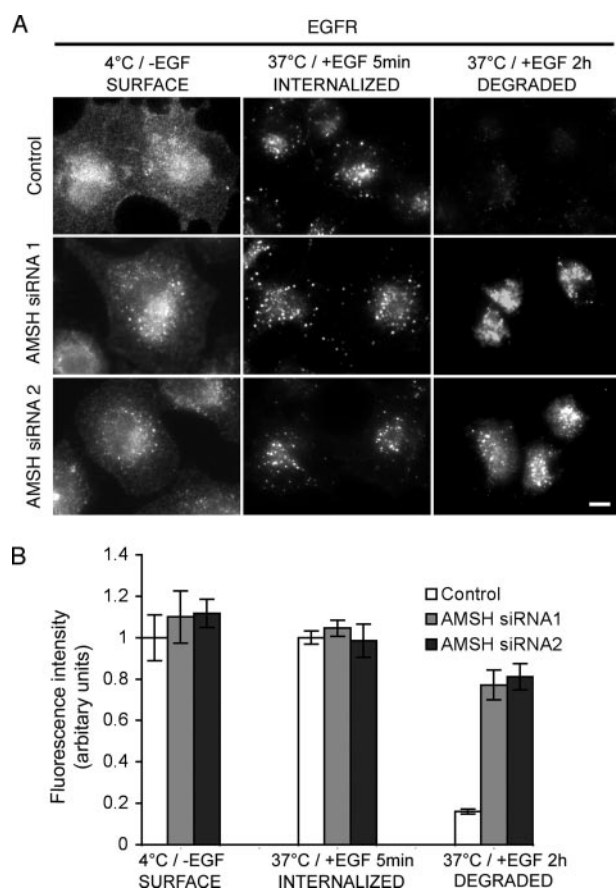
A

FIGURE 6. AMSH silencing by RNA interference inhibits EGFR degradation. *A*, HeLa cells were transfected with either one of two different siRNAs specific for AMSH; 72 h after transfection, the cells were serum-starved, incubated with EGF, and subjected to the same EGFR internalization and degradation assay as described in the legends for Figs. 4 and 5. Representative images are shown. *Scale bar*, 20 μm. Similar results were obtained with mock-transfected cells or with cells transfected with a control siRNA (not shown), thus ruling out nontarget effects. *B*, quantification of surface staining, internalization, and total EGFR from the immunofluorescent images. 30–50 cells transfected with control (*white*), AMSH siRNA1 (*light gray*), or AMSH siRNA2 (*dark gray*) were used for analysis; the specific fluorescent signal of the EGFR of each cell was determined by removing away the background signal (masking step, Slidebook 4). Data were normalized to the fluorescent signal from the control sample determined at 4 °C. Data corresponds to average ± standard error of the mean. The statistical significance was calculated using the Student's *t* test.

AMSH, such as Vps4 (42), which might result in the inhibition of EGFR degradation. We believe, however, that this is not the case since Vps4E_{228}Q remained associated with the endosomal class E compartment it generates when expressed together with either CHMP3-(151–220) or CHMP3-(151–222) (Fig. 3, *B* and *C*). Thus, endosomal localization of AMSH seems to be important for efficient down-regulation of EGFR. It has been established that human immunodeficiency virus-1 engages the ESCRT system for budding and release of the viral particles from the plasma membrane (4–8). Overexpression of CHMP3 capable of binding AMSH or of an AMSH mutant unable to remove ubiquitin strongly prevents viral budding, indicating that like degradation of activated EGFR, these virus-associated processes also depend on the correct interaction of CHMP3 with AMSH (34, 43).

Our results concerning the role of endosomal AMSH on EGFR degradation are at variance with the moderate accelera-

tion in receptor degradation previously observed by knocking down AMSH using siRNA (15, 19). The results from our RNA interference experiments, using two different siRNAs specific for AMSH, is a strong inhibition on EGFR degradation. Perhaps one explanation for the differences can be ascribed to the longer post-transfection period (72 *versus* 48 h) used by us to ensure maximum depletion of AMSH.

Our observations do not address whether endosomal AMSH acts directly on cargoes, on components of the ESCRT machinery, or on both. UBPY is another mammalian STAM-binding deubiquitinating enzyme targeted to endosomes. It was recently shown that changes in the expression level of UBPY but not of AMSH affects the ubiquitination level of EGFR, suggesting that EGFR is not a substrate of AMSH (18). STAM appears to be a substrate for the deubiquitinating activity of AMSH, however, as expression of an enzymatically inactive form of AMSH (D348A) increased the amount of ubiquitinated STAM and enhanced the association of AMSH with endosomes (15, 39). Thus, it remains a possibility that the mislocalization of AMSH attained during our experiments slows down the deubiquitination of STAM and thereby accelerates its own degradation and prevents EGFR degradation. Indeed, knocking down of UBPY expression results in accelerated degradation of STAM and inhibition of EGFR degradation (20).

In summary, AMSH interacts with a least three distinct components of the MVB pathway, STAM, CHMP3, and clathrin. Proper endosomal localization of AMSH is required for efficient EGFR degradation but not for its internalization. Presumably, other membrane proteins, also using ubiquitin as a sorting signal to enter the MVB pathway, are similarly dependent on AMSH for their degradation.

Addendum—When this manuscript was in preparation, the CHMP3-AMSH interaction was independently reported by McCullough *et al.* (39).

REFERENCES

1. Raiborg, C., Bache, K. G., Mehlum, A., Stang, E., and Stenmark, H. (2001) *EMBO J.* **20,** 5008–5021
2. Sigismund, S., Polo, S., and Di Fiore, P. P. (2004) *Curr. Top. Microbiol. Immunol.* **286,** 149–185
3. Babst, M. (2005) *Traffic* **6,** 2–9
4. Garrus, J. E., von Schwedler, U. K., Pornillos, O. W., Morham, S. G., Zavitz, K. H., Wang, H. E., Wettstein, D. A., Stray, K. M., Cote, M., Rich, R. L., Myszka, D. G., and Sundquist, W. I. (2001) *Cell* **107,** 55–65
5. Martin-Serrano, J., Zang, T., and Bieniasz, P. D. (2001) *Nat. Med.* **7,** 1313–1319
6. Strack, B., Calistri, A., Craig, S., Popova, E., and Gottlinger, H. G. (2003) *Cell* **114,** 689–699
7. von Schwedler, U. K., Stuchell, M., Muller, B., Ward, D. M., Chung, H. Y., Morita, E., Wang, H. E., Davis, T., He, G. P., Cimbora, D. M., Scott, A., Krausslich, H. G., Kaplan, J., Morham, S. G., and Sundquist, W. I. (2003) *Cell* **114,** 701–713
8. Morita, E., and Sundquist, W. I. (2004) *Annu. Rev. Cell Dev. Biol.* **20,** 395–425
9. Reggiori, F., and Pelham, H. R. (2001) *EMBO J.* **20,** 5176–5186
10. Amerik, A. Y., Nowak, J., Swaminathan, S., and Hochstrasser, M. (2000) *Mol. Biol. Cell* **11,** 3365–3380

11. D'Andrea, A., and Pellman, D. (1998) *CRC Crit. Rev. Biochem. Mol. Biol.* **33,** 337–352
12. Amerik, A. Y., and Hochstrasser, M. (2004) *Biochim. Biophys. Acta* **1695,** 189–207
13. Nijman, S. M., Luna-Vargas, M. P., Velds, A., Brummelkamp, T. R., Dirac, A. M., Sixma, T. K., and Bernards, R. (2005) *Cell* **123,** 773–786
14. Naviglio, S., Mattecucci, C., Matoskova, B., Nagase, T., Nomura, N., Di Fiore, P. P., and Draetta, G. F. (1998) *EMBO J.* **17,** 3241–3250
15. McCullough, J., Clague, M. J., and Urbe, S. (2004) *J. Cell Biol.* **166,** 487–492
16. Kato, M., Miyazawa, K., and Kitamura, N. (2000) *J. Biol. Chem.* **275,** 37481–37487
17. Kaneko, T., Kumasaka, T., Ganbe, T., Sato, T., Miyazawa, K., Kitamura, N., and Tanaka, N. (2003) *J. Biol. Chem.* **278,** 48162–48168
18. Mizuno, E., Iura, T., Mukai, A., Yoshimori, T., Kitamura, N., and Komada, M. (2005) *Mol. Biol. Cell* **16,** 5163–5174
19. Bowers, K., Piper, S. C., Edeling, M. A., Gray, S. R., Owen, D. J., Lehner, P. J., and Luzio, J. P. (2006) *J. Biol. Chem.* **281,** 5094–5105
20. Row, P. E., Prior, I. A., McCullough, J., Clague, M. J., and Urbe, S. (2006) *J. Biol. Chem.* **281,** 12618–12624
21. Campbell, R. E., Tour, O., Palmer, A. E., Steinbach, P. A., Baird, G. S., Zacharias, D. A., and Tsien, R. Y. (2002) *Proc. Natl. Acad. Sci. U. S. A.* **99,** 7877–7882
22. Ogawa, H., Ishiguro, K., Gaubatz, S., Livingston, D. M., and Nakatani, Y. (2002) *Science* **296,** 1132–1136
23. Shi, Y., Sawada, J., Sui, G., Affar el, B., Whetstine, J. R., Lan, F., Ogawa, H., Luke, M. P., and Nakatani, Y. (2003) *Nature* **422,** 735–738
24. Massol, R. H., Larsen, J. E., Fujinaga, Y., Lencer, W. I., and Kirchhausen, T. (2004) *Mol. Biol. Cell* **15,** 3631–3641
25. Burke, P., Schooler, K., and Wiley, H. S. (2001) *Mol. Biol. Cell* **12,** 1897–1910
26. Ward, D. M., Vaughn, M. B., Shiflett, S. L., White, P. L., Pollock, A. L., Hill, J., Schnegelberger, R., Sundquist, W. I., and Kaplan, J. (2005) *J. Biol. Chem.* **280,** 10548–10555
27. Whitley, P., Reaves, B. J., Hashimoto, M., Riley, A. M., Potter, B. V., and Holman, G. D. (2003) *J. Biol. Chem.* **278,** 38786–38795
28. Bache, K. G., Stuffers, S., Malerod, L., Slagsvold, T., Raiborg, C., Lechardeur, D., Walchli, S., Lukacs, G. L., Brech, A., Stenmark, H., and Schmid, S. (2006) *Mol. Biol. Cell* **17,** 2513–2523
29. Tanaka, N., Kaneko, K., Asao, H., Kasai, H., Endo, Y., Fujita, T., Takeshita, T., and Sugamura, K. (1999) *J. Biol. Chem.* **274,** 19129–19135
30. Shiflett, S. L., Ward, D. M., Huynh, D., Vaughn, M. B., Simmons, J. C., and Kaplan, J. (2004) *J. Biol. Chem.* **279,** 10982–10990
31. Yeo, S. C., Xu, L., Ren, J., Boulton, V. J., Wagle, M. D., Liu, C., Ren, G., Wong, P., Zahn, R., Sasajala, P., Yang, H., Piper, R. C., and Munn, A. L. (2003) *J. Cell Sci.* **116,** 3957–3970
32. Pankratz, N., and Foroud, T. (2004) *NeuroRx* **1,** 235–242
33. Nakamura, M., Tanaka, N., Kitamura, N., and Komada, M. (2006) *Genes Cells* **11,** 593–606
34. Zamborlini, A., Usami, Y., Radoshitzky, S. R., Popova, E., Palu, G., and Göttlinger, H. G. (2006) *Proc. Natl. Acad. Sci. U. S. A.* **103,** 19140–19145
35. Babst, M., Wendland, B., Estepa, E. J., and Emr, S. D. (1998) *EMBO J.* **17,** 2982–2993
36. Fujita, H., Yamanaka, M., Imamura, K., Tanaka, Y., Nara, A., Yoshimori, T., Yokota, S., and Himeno, M. (2003) *J. Cell Sci.* **116,** 401–414
37. Yoshimori, T., Yamagata, F., Yamamoto, A., Mizushima, N., Kabeya, Y., Nara, A., Miwako, I., Ohashi, M., Ohsumi, M., and Ohsumi, Y. (2000) *Mol. Biol. Cell* **11,** 747–763
38. Tsujita, K., Itoh, T., Ijuin, T., Yamamoto, A., Shisheva, A., Laporte, J., and Takenawa, T. (2004) *J. Biol. Chem.* **279,** 13817–13824
39. McCullough, J., Row, P. E., Lorenzo, O., Doherty, M., Beynon, R., Clague, M. J., and Urbe, S. (2006) *Curr. Biol.* **16,** 160–165
40. Luhtala, N., and Odorizzi, G. (2004) *J. Cell Biol.* **166,** 717–729
41. Mizuno, E., Kawahata, K., Okamoto, A., Kitamura, N., and Komada, M. (2004) *J. Biochem.* (*Tokyo*) **135,** 385–396
42. Scott, A., Gaspar, J., Stuchell-Brereton, M. D., Alam, S. L., Skalicky, J. J., and Sundquist, W. I. (2005) *Proc. Natl. Acad. Sci. U. S. A* **102,** 13813–13818
43. Agromayor, M., and Martin-Serrano, J. (2006) *J. Biol. Chem.* **281,** 23083–23091

Targeting of AMSH to Endosomes Is Required for Epidermal Growth Factor Receptor Degradation

Yu May Ma, Emmanuel Boucrot, Judit Villén, El Bachir Affar, Steven P. Gygi, Heinrich G. Göttlinger and Tomas Kirchhausen

Access the most updated version of this article at doi: 10.1074/jbc.M611635200

Alerts:
- When this article is cited
- When a correction for this article is posted

Click here to choose from all of JBC's e-mail alerts

This article cites 42 references, 28 of which can be accessed free at
http://www.jbc.org/content/282/13/9805.full.html#ref-list-1